Effect of Protein Hydration on Receptor Conformation: Decreased Levels of Bound Water Promote Metarhodopsin II Formation

Drake C. Mitchell and Burton J. Litman*

Section of Fluorescence Studies, Laboratory of Membrane Biophysics and Biochemistry, National Institute on Alcohol Abuse and Alcoholism, National Institutes of Health, Rockville, Maryland 20852

Received March 18, 1999; Revised Manuscript Received April 29, 1999

ABSTRACT: Neutral solutes were used to investigate the effects of osmotic stress both on the ability of rhodopsin to undergo its activating conformation change and on acyl chain packing in the rod outer segment (ROS) disk membrane. The equilibrium concentration of metarhodopsin II (MII), the conformation of photoactivated rhodopsin, which binds and activates transducin, was increased by glycerol, sucrose, and stachyose in a manner which was linear with osmolality. Analysis of this shift in equilibrium in terms of the dependence of $\ln(K_{eq})$ on osmolality revealed that 20 ± 1 water molecules are released during the MI-to-MII transition at 20 °C, and at 35 °C 13 ± 1 waters are released. At 35 °C the average time constant for MII formation was increased from 1.20 ± 0.09 ms to 1.63 ± 0.09 ms by addition of 1 osmolal sucrose or glycerol. The effect of the neutral solutes on acyl chain packing in the ROS disk membrane was assessed via measurements of the fluorescence lifetime and anisotropy decay of 1,6-diphenyl-1,3,5-hexatriene (DPH). Analysis of the anisotropy decay of DPH in terms of the rotational diffusion model showed that the angular width of the equilibrium orientational distribution of DPH about the membrane normal was progressively narrowed by increased osmolality. The parameter f_v, which is proportional to the overlap between the DPH orientational probability distribution and a random orientational distribution, was reduced by the osmolytes in a manner which was linear with osmolality. This study highlights the potentially opposing interplay between the effect of membrane surface hydration on both the lipid bilayer and integral membrane protein structure. Our results further demonstrate that the binding and release of water molecules play an important role in modulating functional conformational changes for integral membrane proteins, as well as for soluble globular proteins.

The central role of water in stabilizing biological macromolecules and facilitating their activity is at once obvious and enigmatic. In the field of protein structure, the essential nature of protein−water interactions with respect to the stabilization of protein structure is one of the central paradigms. The general importance of changes in hydration in enzyme activity is widely acknowledged, (*1, 2*) but detailed knowledge regarding how the release or uptake of water molecules may affect the energetics of protein conformational changes is often in short supply. This is particularly true for integral membrane proteins, where variation of membrane hydration induced by changes in water activity may simultaneously alter functionally relevant conformational equilibria of proteins and the physical properties of the phospholipid bilayer. Thus, a complete understanding of the role of membrane hydration in modulating membrane protein function requires the ability to separately analyze the effects of altered surface membrane hydration on both protein function and bilayer physical properties.

Changes in the number of bound water molecules associated with a specific enzymatic process have been measured for several enzymes via the osmotic stress protocol (*3*). This experimental strategy is based on the fact that the water activity of aqueous compartments of proteins, which excludes a solute, is dependent on the concentration of the excluded solute. Inaccessibility to solute may be due to either the topology of the protein or the protein's 'hydration shell', as defined by Arakawa and Timasheff (*4*). The result is that the presence of an osmotically active solute inhibits protein conformational changes in which there is a net uptake of water and favors processes in which a protein releases water to the bulk aqueous medium. The osmotic stress strategy has been used to measure the net change in the number of bound water molecules involved in the functional conformational changes of hemoglobin (*5*, *6*), hexokinase (*7*, *8*), adenosine deaminase (*9*), and aspartate transcarbamylase (*10*). These soluble, and in some cases multicomponent, enzymes undergo large conformational changes in order to bind substrate; thus, it is not surprising that energies associated with changes in solvation play a significant role in determining their functional efficacy. For integral membrane receptors, which may have only half of their surface exposed to the aqueous phase and are imbedded in a phospholipid bilayer, it is not obvious how significant changes in solvation may affect functional activity. Osmotic stress studies on potassium channels (*11*), alamecithin (*12*), sodium channels (*13*), and cytochrome *c* oxidase (*14*) have detected changes in the number of water molecules associated with these membrane proteins as they undergo functional conformation changes.

* Corresponding author: Park Building, Room 158, 12420 Parklawn Dr., Rockville, MD 20852. Email: litman@helix.nih.gov. Phone: 301-594-3608. Fax: 301-594-0035.

10.1021/bi990634m
Published on Web 05/26/1999

Changes in water associated with the surface of model membranes alter phospholipid bilayer properties in ways that have been shown to have functional consequences (see *15* for a review). Lowered water activity leads to increased phospholipid acyl chain packing with a concomitant reduction in bilayer free volume (*16*), and this effect has been correlated with decreased rates of electron transport by diffusion of quinones in mitochondrial and chloroplast membranes (*17*). Fluorescence recovery after photobleaching measurements in PC[1] multibilayers show that reduced water content decreases the lateral diffusion coefficient of phospholipids (*18*).

We report here the effects of osmotic stress both on the activating conformational change of the G protein-coupled receptor rhodopsin and on the acyl chain packing of the ROS disk membrane. Rhodopsin is an ideal receptor for studying the role of hydration in membrane receptor function because of the relative abundance of structural information that is available both within the membrane (*19, 20*) and in the region exposed to the cytoplasm (*21*). About 50% of rhodopsin is exposed to water, and about half of the exposed protein surface is on the cytoplasmic face of the molecule where transducin and a number of regulatory proteins bind rhodopsin at various times during visual signal transduction (*22*). A metastable equilibrium between the MI and MII conformational states is established within a few milliseconds of photon absorption (*23*). The principal protein conformational change of photolyzed rhodopsin occurs during the transition from MI to MII. MII is the conformation which binds and activates the visual G protein, transducin (*24*). A large number of the structural details involved in the MI-to-MII conformational change have been elucidated (*22*), including changes in the hydrogen bonding of internal water molecules (*25, 26*). In addition, the dependence of the MI−MII equilibrium on bilayer composition (*27*−*29*) and physical properties of the lipid bilayer (*30*−*32*) is well characterized. Rhodopsin constitutes at least 95% of the disk membrane protein, so that the interpretation of rhodopsin−lipid interactions is not complicated by the presence of other proteins.

EXPERIMENTAL METHODS

Sample Preparation. Intact ROS disks were prepared from frozen bovine retinas as previously described (*33*). Stachyose was purchased from Sigma Chemicals, and DPH was purchased from Molecular Probes Inc. Samples for all studies (8 μM rhodopsin for all absorbance measurements, 1.2 μM rhodopsin for fluorescence measurements) were prepared in a low-salt buffer (10 mM HEPES, 50 μM DTPA, pH 7.5) with the required solute. Solute-containing samples were then put through 10 freeze−thaw cycles to ensure that the solute had equilibrated across the membrane and, immediately prior to use, were extruded through a 0.2 μm pore filter 10 times to reduce scattered light. All procedures were carried out under argon in a glovebox to minimize oxidation of the polyunsaturated acyl chains of the ROS disk membrane. The osmolality of all solutions was determined with a Wescor Vapro 5520 vapor pressure osmometer.

Equilibrium Absorbance Measurements. Absorbance spectra of MI−MII equilibrium mixtures ~3s following a flash which bleached 15−20% of the rhodopsin were acquired with a Hewlett-Packard 8452A diode array spectrophotometer (0.2 s measurements yielded <0.3% bleach by the measuring beam) (*34*). Individual MI and MII bands were resolved by using nonlinear least squares to fit the sum of two asymmetric Gaussian absorbance bands to difference spectra which had been corrected for the presence of unbleached rhodopsin (*34*). The equilibrium constant for the MI to MII conversion is defined by K_{eq} = [MII]/[MI]. The change in free energy, $\Delta(\Delta G)$, for the MI−MII equilibrium due to the presence of the solutes was calculated according to

$$\Delta(\Delta G) = \Delta G_{solute} - \Delta G_{control} \quad (1)$$

The effect of osmotic stress on the MI−MII equilibrium was analyzed using established thermodynamic relationships (*3*). The change in the number of water molecules in solute-inaccessible regions, ΔN_w, is given by the slope of a line relating $\ln(K_{eq})$ and the osmolal solute concentration:

$$\ln (K_{eq}) = -\Delta N_w \times \frac{[\text{osmolal}]}{55.6} \quad (2)$$

Kinetic Absorbance Measurements. The absorbance at 380 nm was monitored with an OLIS RSM-1000 rapid-scanning spectrophotometer operating in the single-wavelength mode. Absorbance readings were acquired every 100 μs for 100 ms. The activating flash, provided by a flashlamp, bleached 7−9% of the rhodopsin. Sheet polarizers in the flash and measuring beams polarized the flash at 54.7° relative to the polarized measuring beam. The increase in absorbance at 380 nm was well described by the sum of two exponentials.

Fluorescence Measurements and Analysis. Fluorescence lifetime and differential polarization measurements were performed with an ISS K2 multifrequency cross-correlation phase fluorometer. Excitation at 351 nm was provided by an argon ion laser. Lifetime and differential polarization data were acquired using decay acquisition software provided by ISS, using 12 or 15 modulation frequencies, logarithmically spaced from 5 to 250 MHz. Scattered excitation light was removed from the emission beam by a 390 nm highpass filter. All lifetime measurements were made with the emission polarizer at the magic angle of 54.7° relative to the vertically polarized excitation beam and with POPOP in absolute ethanol in the reference cuvette. For each differential polarization measurement, the instrumental polarization factors were measured and found to be between 1 and 1.05, and the appropriate correction factor was applied. At each frequency, data were accumulated until the standard deviations of the phase and modulation ratio were below 0.2° and 0.004, respectively, and these values were used as the standard deviation for the measured phases and modulation ratios in all subsequent analysis. Both total intensity decay and differential polarization measurements were repeated a minimum of 3 times.

Total fluorescence intensity decays were modeled with two Lorentzian distributions, plus a discrete exponential decay.

[1] Abbreviations: ROS, rod outer segment; DPH, 1,6-diphenyl-1,3,5-hexatriene; MI, metarhodopsin I; MII, metarhodopsin II; DTPA, diethylenetriaminepentaacetic acid; LC, liquid crystalline; PC, phosphatidylcholine; PIPES, piperazine-*N*,*N*′-bis(2-ethanesulfonic acid); POPOP, 1,4-bis(5-phenyloxazol-2-yl)benzene; BRD, Brownian rotational diffusion.

The lifetime of the discrete component was fixed at 0.001 ns, and its fractional intensity was allowed to vary along with the centers of the two Lorentzian distributions, $\tau_{Lor\ 1}$ and $\tau_{Lor\ 2}$, and the widths of the distributions at half-height, w_1 and w_2. The resulting fractional intensity of the discrete component varied from 0.8% to less than 0.1%, and the values of reduced χ^2 ranged from 1 to 5.

Measured polarization-dependent differential phases and modulation ratios for each sample were combined with the measured total intensity decay to yield the anisotropy decay, $r(t)$. All anisotropy decay data were analyzed using the BRD model as previously described (*35*). The results of the BRD model-based analysis were interpreted in terms of an angular distribution function which is symmetric about $\theta = \pi/2$:

$$f(\theta) = N^{-1} \exp[\lambda_2 P_2(\cos\theta) + \lambda_4 P_4(\cos\theta)] \qquad (3)$$

where $P_2(\cos\theta)$ and $P_4(\cos\theta)$ are the 2nd and 4th Legendre polynomials, λ_2 and λ_4 are constants determined by simultaneous solution of equations for the order parameters $\langle P2\rangle$ and $\langle P4\rangle$, and N is the normalization constant determined according to

$$N = \int_0^{\pi} \sin(\theta) \exp[\lambda_2 P_2(\cos\theta) + \lambda_4 P_4(\cos\theta)]\, d\theta \qquad (4)$$

The extent to which the equilibrium orientational freedom of DPH is restricted by the phospholipid acyl chains was quantified using the parameter f_v (*36*), which is defined by

$$f_v = \frac{1}{2 \times f(\theta)_{max}} \qquad (5)$$

All data analyses were performed with NONLIN (*37*), with all subroutines specifying the fitting functions written by the authors. Asymmetric confidence intervals corresponding to 1 standard deviation were obtained by NONLIN for both fitting variables and derived parameters.

RESULTS

Effect of Solutes on MI−MII Equilibrium. The presence of the neutral solutes resulted in a shift in the MI−MII equilibrium toward MII. To compare the relative strength of the solute effects on the MI−MII equilibrium at two different temperatures, the shifts in K_{eq} were converted to changes in the change in free energy, $\Delta(\Delta G)$ (see eq 1). Increasing solute concentration made $\Delta(\Delta G)$ more negative, in a unique manner for each solute, as shown by the data obtained at 20 °C in Figure 1A. When the molar solute concentrations were converted to osmolal concentrations, a single, linear dose−response relationship was obtained for all of the solutes at each temperature (Figure 1B) (20 °C data), demonstrating that the shift in the MI−MII equilibrium is due to altered water activity.

The change in the number of bound water molecules between MI and MII was obtained by analyzing plots of ln(K_{eq}) vs osmolality (Figure 1C). The slopes of the lines in Figure 1C indicate that 20 ± 1 and 13 ± 1 water molecules are released during the MI to MII transition, and at 20 and 35 °C, respectively. The lines in Figure 1C were determined using NONLIN; thus, the error estimates for ΔN_w are based on the propagated errors for the individual determinations of K_{eq}. The change in the number of water molecules released

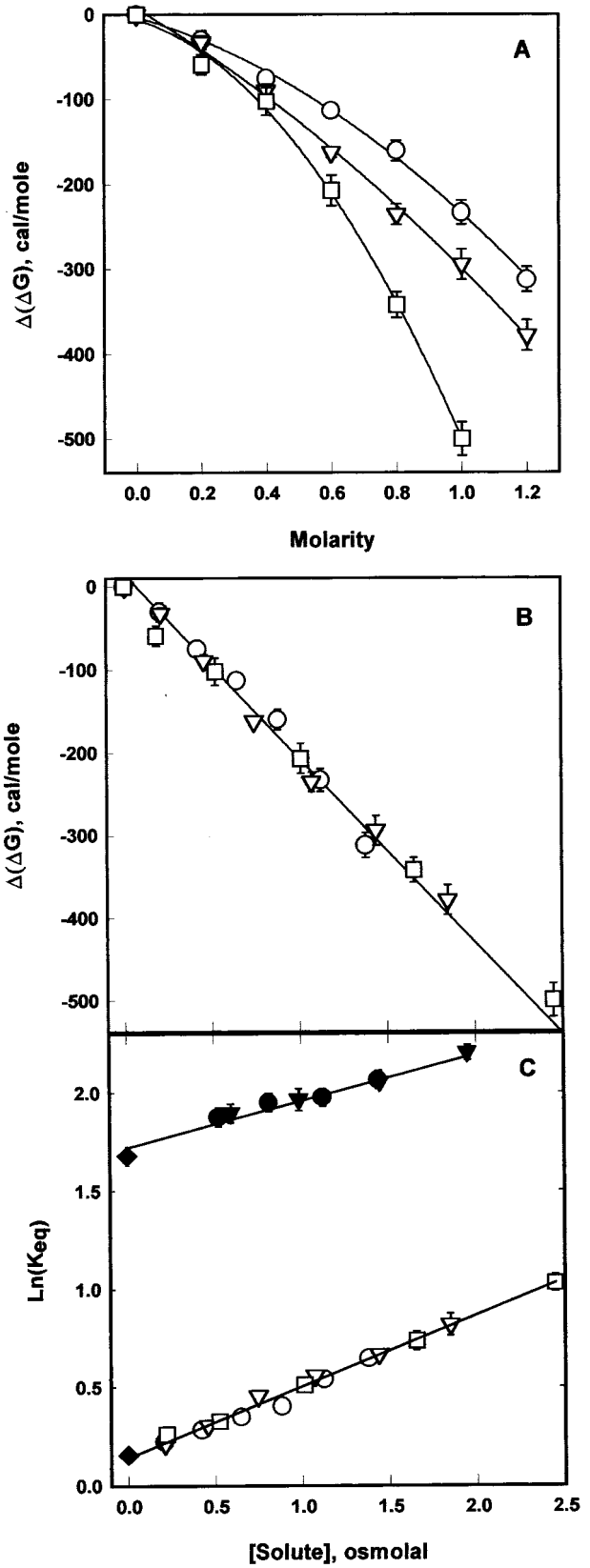

FIGURE 1: Effects of solute molarity (A) and osmolality (B) on ΔG for the MI ⇒ MII transition, with $\Delta(\Delta G)$ calculated according to eq 1. (C) Analysis of the effects of solute on K_{eq} for the MI−MII equilibrium at 20 and 35 °C in terms of eq 2; the slope of each line equals $-\Delta N_w/55.6$. (○) Glycerol, 20 °C; (▽) sucrose, 20 °C; (□) stachyose, 20 °C; (●) glycerol, 35 °C; (▼) sucrose, 35 °C; (◆) control, both temperatures.

upon MII formation with temperature indicates that there is an entropic contribution to the change in free energy associated with the release of water molecules. It was determined from the dependence of $\Delta(\Delta G)$ on osmolality (Figure 1B) that at 20 °C, $\Delta(\Delta G)_{os} = -223$ cal mol^{-1} Os^{-1} and at 35 °C $\Delta(\Delta G)_{os} = -170$ cal mol^{-1} Os^{-1}. Substituting $\Delta G_{os} = \Delta H_{os} - T\Delta S_{os}$ and solving these two equations for ΔS_{os} and ΔH_{os} yielded $\Delta S_{os} = -3.4$ cal mol^{-1} K^{-1} Os^{-1} and $\Delta H_{os} = -1.2$ kcal mol^{-1} Os^{-1} for the entropic and enthalpic contributions to the difference in free energy between the release of water molecules into the solute-containing solution and one with no added solute.

Effect of Solutes on Kinetics of MII Formation. Sucrose and glycerol slowed the rate of formation of MII, as determined from the flash-induced change in absorbance at 380 nm. The smooth curves in Figure 2A show the results of fitting an empirical sum-of-2-exponentials function to the kinetic data, and the residuals for the control sample (Figure 2B) show that this is an accurate description of the kinetic data. Increasing the concentration of glycerol or sucrose caused an increase in both $\tau 1$ and $\tau 2$. Under all osmotic conditions, approximately 70% of the absorbance increase at 380 nm was associated with the shorter time constant, $\tau 1$. On a relative basis, $\tau 1$ was increased by osmolality about twice as much as $\tau 2$, as shown by the steeper corrrelation line for $\ln(\tau 1)$ vs osmolality in Figure 2C. Over the range of osmolalities investigated, $\tau 1$ was increased by a factor of 2, while $\tau 1$ was increased by 50%.

Effect of Solutes on DPH Fluorescence. The high concentration of rhodopsin in the ROS disk membrane (1 rhodopsin per 75 phospholipids) results in substantial quenching of the DPH fluorescence due to energy transfer to the retinal chromophore. The best analysis of the DPH fluorescence lifetime was obtained using the sum of two Lorentzian distributions plus a minor discrete component. At 20 °C, in the absence of solutes, 66% of the DPH fluorescence intensity was centered at 7.3 ± 0.2 ns in a narrow Lorentzian distribution ($w_1 = 0.2 \pm 0.1$ ns) and 33% was centered at 2.5 ± 0.3 ns in a very broad Lorentzian distribution ($w_2 = 2.0 \pm 0.6$ ns). At 35 °C the centers of the distributions moved to 5.9 ± 0.6 and 1.7 ± 0.4 ns, respectively, and the distribution widths and fractional contributions were essentially unchanged. At both temperatures, all of the solutes (glycerol, sucrose, and stachyose at 20 °C and sucrose at 35 °C) had very little effect on the widths or centers of the two Lorentzian distributions.

In contrast with the total fluorescence intensity decay, the decay of fluorescence anisotropy, $r(t)$, was quite sensitive to the concentration of added solute. The BRD model characterizes $r(t)$ in terms of the equilibrium orientational distribution of the probe, $f(\theta)$, and the rotational diffusion coefficient, $D_\perp$ (*35*). At both 20 °C and 35 °C, the solutes caused a moderate reduction of $D_\perp$ in a manner that was correlated with osmolality (data not shown). The solutes had a larger effect on the DPH orientational probability distribution, $f(\theta) \sin \theta$, as shown in Figure 3A. The nature of the solute-induced changes in $f(\theta) \sin \theta$ is apparent from the difference curves in Figure 3B, where $f(\theta) \sin \theta$ obtained in the absence of solute has been subtracted from the three curves for solute-containing samples. Areas below the zero line in Figure 3B correspond to angular orientations from which the DPH is excluded in the presence of solute, and areas above the zero line denote angular orientations that are preferentially allowed by the bilayer in the presence of solute. The solutes restricted DPH orientations greater than ~20° from the membrane normal, and an increase in the concentration of added solute caused a progressive narrowing of the probability distribution centered about the membrane normal.

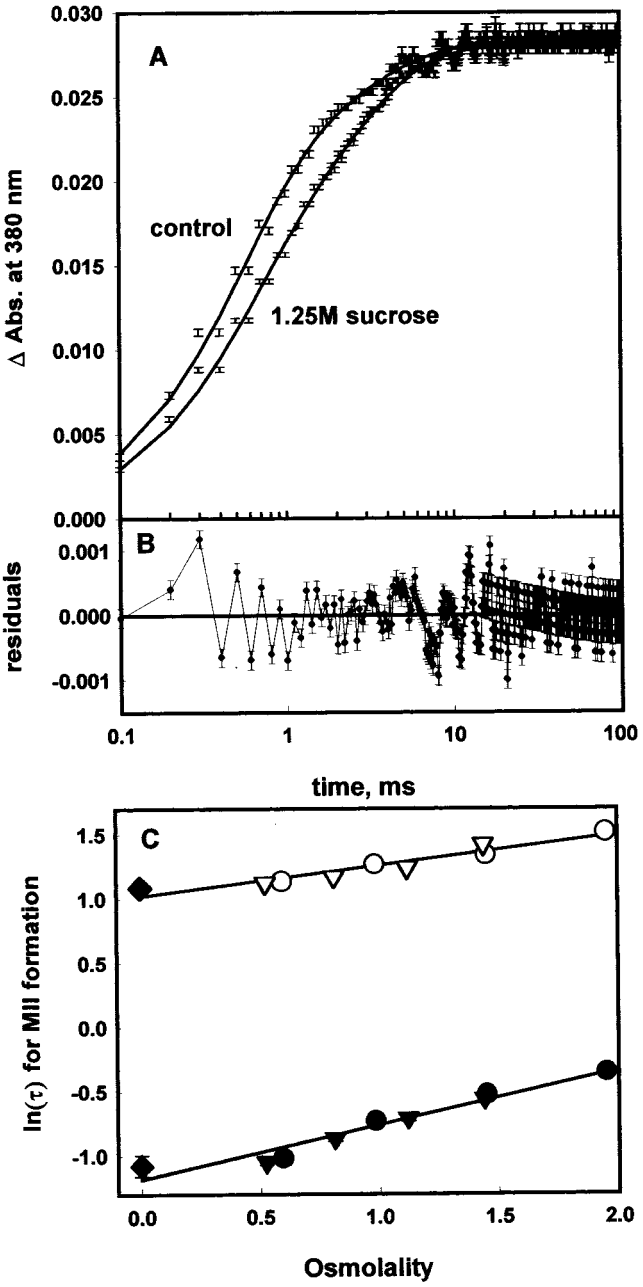

FIGURE 2: Example of the effect of neutral solute on the kinetics of MII formation at 35 °C as monitored by the increase in absorbance at 380 nm. (A) Points with error bars are the increase in absorbance following an actinic flash; smooth curves are the sum-of-2-exponentials fit to the data. (B) Residuals for the control curve in panel A. (C) The two time constants for MII formation, $\tau 1$ and $\tau 2$, as a function of osmolality: (●) $\tau 1$ in glycerol; (▼) $\tau 1$ in sucrose; (○) $\tau 2$ in glycerol; (▽) $\tau 2$ in sucrose; (◆) $\tau 1$ and $\tau 2$ control.

The parameter f_v (eq 5) summarizes the orientational probability distribution of DPH, and previous investigations have shown that this parameter is directly related to the MI−MII equilibrium constant (*30*−*32*). All of the solutes, at both

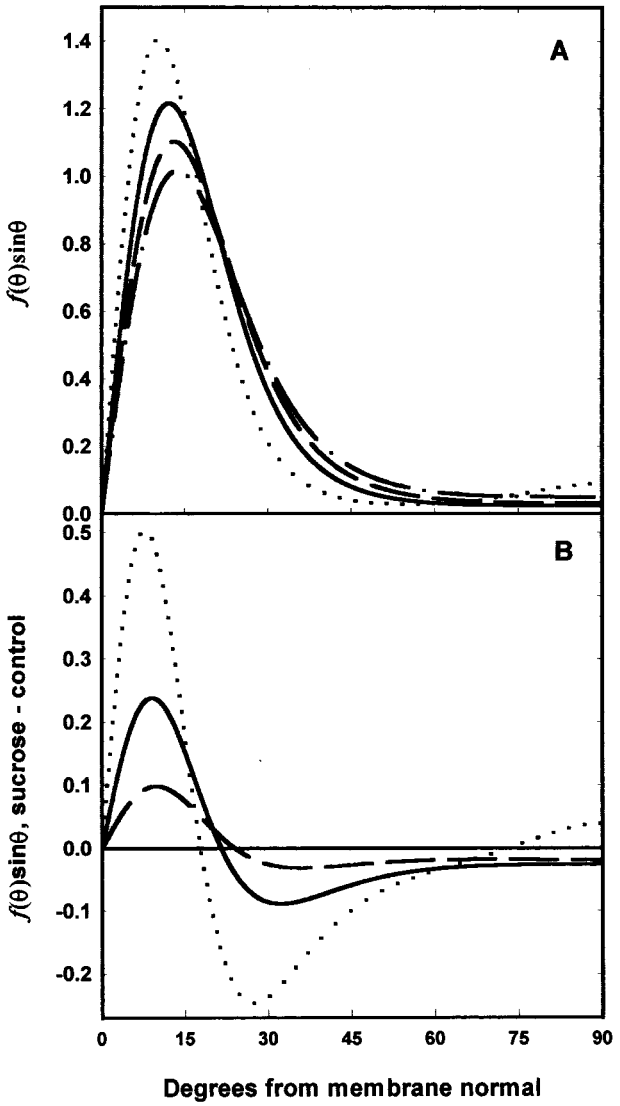

FIGURE 3: (A) Examples of the effect of neutral solutes on the DPH orientational probability distribution, $f(\theta) \sin \theta$. (B) Difference curves showing the net change in $f(\theta) \sin \theta$ due to the presence of neutral solute. The solute induces a shift in the DPH orientational distribution away from regions below the zero line into regions above the zero line. (− · −) Control; (− −) 0.5 M sucrose; (—) 1.0 M sucrose; (···) 1.5 M sucrose.

temperatures, lowered f_v in a manner which was nonlinear in molarity (Figure 4A) but linear in osmolality (Figure 4B). The two linear correlations in Figure 4B demonstrate that acyl chain packing in the ROS disk membrane is altered by solution osmolality, and the magnitude of the alteration is increased with increasing temperature. Thus, solution osmolality orders acyl chain packing, lowers f_v, and simultaneously increases the equilibrium concentration of MII.

DISCUSSION

A number of investigations have shown that the MI−MII equilibrium is quite sensitive to changes in acyl chain packing in the surrounding phospholipid bilayer (*30*−*32*). Thus, an obvious question is whether the observed solute-induced changes in K_{eq} and MII kinetics are simply a consequence of solute-induced changes in phospholipid acyl chain packing. Previously we have shown that factors which increase K_{eq}, increased temperature (*30*−*32*), increased acyl chain

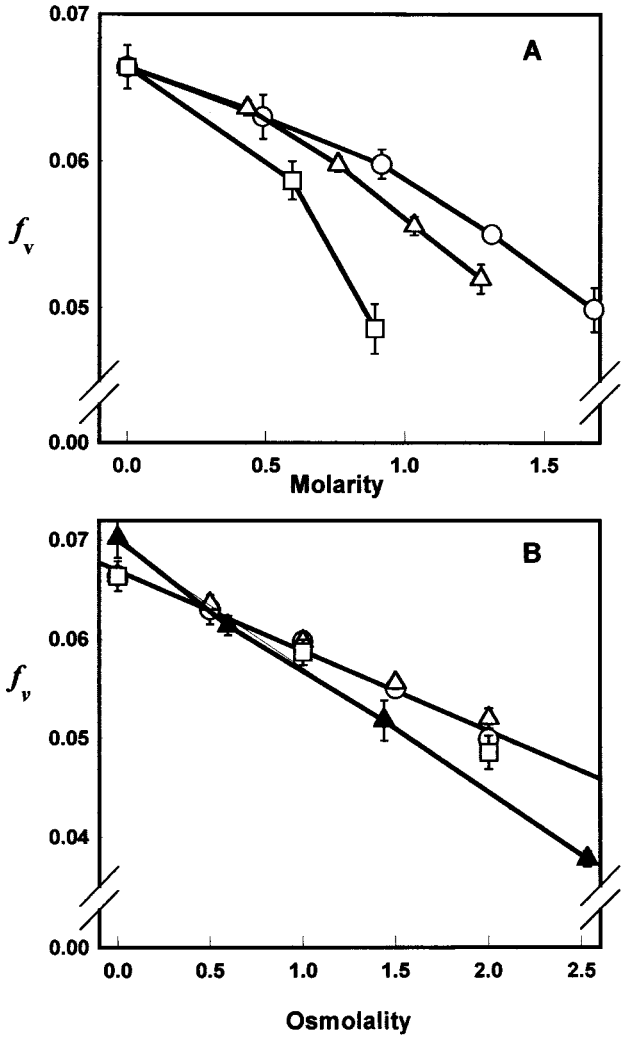

FIGURE 4: Effect of solute molarity (A) and osmolality (B) on the parameter f_v at 20 and 35 °C. (○) Glycerol, 20 °C; (△) sucrose, 20 °C; (□) stachyose, 20 °C; (▲) sucrose, 35 °C.

unsaturation (*31*, *32*), decreased bilayer cholesterol (*30*, *31*), also increase f_v and changes in these two parameters are linearly related. However, osmotic stress simultaneously raises K_{eq} (Figure 1) and lowers f_v (Figure 4). The augmentation of MII formation by osmotically active solutes is coupled with increased acyl chain packing, which has been shown to reduce MII formation. This leads us to conclude that the solute-induced shift in MI−MII is not mediated by the phospholipid acyl chain packing in the ROS disk membrane, but is related to changes in the hydration of rhodopsin itself.

The neutral solutes glycerol, sucrose, and stachyose all had identical effects on MII kinetics and equilibrium concentration when their concentration is stated in terms of osmolality or osmotic stress. When physically dissimilar substances produce identical effects, the usual interpretation is that the solutes are acting on enzyme activity indirectly by altering water activity (*3*). Thus, we propose that all three solutes alter the MI-to-MII conformational change due to an osmotic effect, that is, because of a difference in the number of solute-excluded water molecules associated with the MI and MII conformations. The identical effects of glycerol (MW = 92) and stachyose (MW = 666) indicate that the regions of rhodopsin where hydration is altered are equally inaccessible to these two solutes which differ in size

by a factor of 7. This indicates that the hydration-sensitive region of rhodopsin is similar to that of hemoglobin (*5*) and the catalytic subunit of aspartate transcarbamylase (*10*), where neutral solutes as small as glycerol had an effect on protein conformational equilibria, which depended solely on osmotic pressure. The lack of a dependence on solute size for rhodopsin implies that the osmotically sensitive regions of rhodopsin must be very narrow crevices or pockets, which expel water during the MI-to-MII transition (*3*). Formation of MII is accompanied by an increase in hydrogen bonding of one or two internal water molecules (*25*); thus, it is unlikely that the pockets that release water molecules are in the protein interior. The cytoplasmic surface of rhodopsin undergoes significant structural rearrangement between MI and MII, and this is the most likely region for small pockets, which undergo a net loss of water during MI ⇒ MII. Near physiological temperature, only 13 ± 1 water molecules are released during MI ⇒ MII. One possibility is that some of these waters are hydrogen bonded to MI, but are released during the MI ⇒ MII transition, with the subsequent formation of new intramolecular hydrogen bonds. This would be consistent with the reported reduction in the number of hydrogen-bonded water molecules accompanying the MI to MII transition (*38*).

The effect of osmotic stress on the MI−MII equilibrium provides a clear example of the fundamental difference between hydrostatic pressure and the osmotic pressure due to exclusion of solutes from an aqueous compartment or region. Increased hydrostatic pressure inhibits the formation of MII, pushing the MI−MII equilibrium toward MI (*39*, *40*). The fundamental difference between hydrostatic and osmotic pressure is most apparent when the response of the system under investigation is considered. A system will be shifted toward minimal volume in response to increased hydrostatic pressure, whereas it will shift toward minimal bound water in response in osmotic pressure (*41*). Hydrostatic pressure alters processes in which there is a change in the total volume of the solution due to a transition between two states. However, water movement that does not produce a density change will be unaltered by hydrostatic pressure. The osmotic stress method is sensitive to all changes in protein solvation because the solute moves water from solute-inaccessible regions to solute-accessible regions. Thus, osmotic stress reveals the difference in solvation between two protein conformations whether there is a difference in total density for the two conformations. Other instances of hydrostatic and osmotic pressure having opposite effects on a protein conformational equilibrium have been reported. One example is poly(L-lysine) where osmotic stress converts α-helical structure to β sheet, where the surface is less hydrated, but hydrostatic pressure favors formation of the more compact α-helical structure (*42*).

The effects of osmotic stress on the kinetics of MII formation are quite different from those observed for the M state of bacteriorhodopsin (*43*). The M state is analogous to MII because both are the only intermediates in their respective photointermediate cascades in which the Schiff base linkage to the retinal chromophore is unprotonated. In bacteriorhodopsin, osmotic stress slowed the decay of M, but had no effect on its formation (*43*). In other words deprotonation of the Schiff base was unaffected, but reprotonation was altered. In contrast, the present results show that in rhodopsin deprotonation of the Schiff base is slowed by osmotic stress. This is consistent with the suggestion that in rhodopsin a single water molecule acts as an intermediary for the transfer of the proton from the Schiff base nitrogen to E113 (*44*), while no involvement of water molecules in the Schiff base deprotonation pathway of bacteriorhodopsin has been detected.

A comparison of the present results with those obtained from a detailed examination of the MI−MII equilibrium as a function of temperature shows the significant contribution of solvation energy to the MI to MII conformational change. The thermodynamic parameters associated with the release of water molecules upon MI ⇒ MII, ΔH_{os} and ΔS_{os}, were determined from the temperature dependence of ΔG_{os}. The result is $\Delta H_{os} = -1.2$ kcal mol^{-1} Os^{-1} and $\Delta S_{os} = -3.2$ cal mol^{-1} K^{-1} Os^{-1}. We previously determined that the change in enthalpy, ΔH, for the MI−MII equilibrium is 10.6 ± 0.5 kcal mol^{-1} and the change in entropy, ΔS, is 37.9 ± 1.8 cal mol^{-1} K^{-1} (*34*). Thus, changes in enthalpy and entropy associated with the release of water molecules into a 1 osmolal solution relative to a 0 osmolal solution are about 10% in magnitude and opposite in sign of those for the overall MI to MII transition. These parameters quantify the two main features of the effect of osmolality on the MI−MII equilibrium; at a fixed temperature, increased osmolality pushes the equilibrium toward MII, and at a fixed osmolality, increased temperature reduces the osmolality-dependent shift toward MII.

The relationship between f_v and K_{eq}, observed for changes in temperature and bilayer cholesterol content, suggests that the measured solute-induced changes in K_{eq} may understate the extent to which solution osmolality alters the equilibrium concentration of MII. If the decrease in acyl chain packing free volume induced by the solutes (Figure 4) reduces MII, as previously reported (*22*), then the observed increased equilibrium concentration of MII is the net result of the antagonistic effects of increased protein dehydration and reduced acyl chain packing free volume. The change in free energy (ΔG) for the MI−MII equilibrium due to a 1 osmolal solution is −220 cal mol^{-1} at 20 °C, as shown in Figure 1B. An osmolality of 1 also lowers f_v by ∼0.007, which would be expected to change ΔG by +150 cal mol^{-1}, according to the relationship between K_{eq} and f_v determined by variation in temperature (*22*). Thus, the osmolality-induced change in acyl chain packing implies that the true effect of a 1 osmolal solution on ΔG for the MI−MII equilibrium at 20 °C may be −370 cal mol^{-1}. At 35 °C a similar estimate of the effect of the solute-induced reduction in f_v leads to a 'corrected' value for ΔG of −400 cal mol^{-1} for a 1 osmolal solution. By correcting all of the values of K_{eq} in Figure 1C for the solute-induced reduction in f_v, it is possible to estimate the change in hydration accompanying the MI ⇒ MII transition in the absence of effects of the solutes on acyl chain packing. Analysis of the 'corrected' equilibrium constants in terms of eq 2 leads to $\Delta N_w = 34 \pm 2$ at 20 °C and $\Delta N_w = 36 \pm 2$ at 35 °C. Within experimental error, these values are identical, suggesting that the difference in hydration between MI and MII is independent of temperature. This result is consistent with the modest structural changes that would be expected when comparing the structures at 20 and 35 °C, and underlines the importance of accounting for the effects of the neutral solutes on acyl

chain packing when dealing with integral membrane proteins.

The osmolality-induced narrowing of the DPH orientational probability distribution (Figure 3) and reduction of the parameter f_v (Figure 4) quantitatively demonstrate the increase in acyl chain packing order and associated reduction in acyl chain packing free volume with decreased water activity. A reduction in membrane free volume with osmotic stress has previously been observed with excimer-forming fluorescent phospholipids (*16*) and in a study of quinone migration as a function of osmotic stress (*17*). The significance of this effect of osmotic stress on acyl chain packing in the present study is that increased acyl chain packing has been observed to reduce the equilibrium concentration of MII. Thus, by combining prior knowledge of how membrane physical properties modulate MII formation with studies of the effect of osmotic pressure on acyl chain packing, it is possible to unambiguously discern which aspects of osmotic stress directly affect the conformational equilibrium of the receptor. In the case of rhodopsin, MII is strongly favored by increased osmotic stress, due to the loss of bound water upon MII formation; this is energetically favorable enough to overcome the inhibiting effect of increased acyl chain packing order on MII formation. Receptors such as rhodopsin, which have their agonist/antagonist binding site in a region of the protein, which is within the membrane, can be very sensitive to the composition and physical properties of the surrounding phospholipid bilayer. However, these studies highlight the need to simultaneously measure both changes in the physical properties of the membrane bilayer and protein function, to distinguish direct effects on the protein from those mediated by changes in the membrane lipid.

REFERENCES

1. Franks, F., and Mathias, S., Eds. (1982) *Biophysics of Water* Wiley, New York.
2. Timasheff, S. N. (1993) *Annu. Rev. Biophys. Biomol. Struct. 22*, 67.
3. Parsegian, V. A., Rand, R. P., and Rau, D. C. (1995) *Methods Enzymol. 259*, 43.
4. Arakawa, T., and Timasheff, S. N. (1985) *Biochemistry 24*, 6536.
5. Colombo, M. F., Rau, D. C., and Paresegian, V. A. (1992) *Science 256*, 655.
6. Colombo, M. F., Rau, D. C., and Paresegian, V. A. (1994) *Proc. Natl. Acad. Sci. U.S.A. 91*, 10517.
7. Rand, R. P., Fuller, N. L. Butko, P., Francis, G., and Nicholls, P. (1993) *Biochemistry 32*, 5925.
8. Reid, C., and Rand, R. P. (1997) *Biophys. J. 72*, 1022.
9. Dzingeleski, G. D., and Wolfenden, R. (1993) *Biochemistry 32*, 9143.
10. LiCata, V. J., and Allewell, N. M. (1997) *Biochemistry 36*, 10161.
11. Zimmerberg, J., Benzanilla, F., and Parsegian, V. A. (1990) *Biophys. J. 57*, 1049.
12. Vodanoy, I., Bezrukov, S. M., and Parsegian, V. A. (1993) *Biophys. J. 63*, 2097.
13. Rayner, M. D., Starkus, J. G., Ruben, P. C., and Alicata, D. A. (1992) *Biophys. J. 61*, 96.
14. Kornblatt, J. A., and Hui Bon Hoa, G. (1990) *Biochemistry 29*, 9370.
15. Blume, A. (1996) *Curr. Opin. Collpod and Interface Sci. 1*, 64.
16. Lehtonen, J. Y. A., and Kinnunen, K. J. (1994) *Biophys. J. 66*, 1981.
17. Mathai, J. C., Sauna, Z. E., Oswald, J.;and Sitaramam, V. (1993) *J. Biol. Chem. 268*, 15442.
18. McCown, J. T., Evans, E., Diehl, S., and Wiles, H. C. (1981) *Biochemistry 20*, 3134.
19. Shertler, G. F. X., and Hargrave, P. A. (1995) *Proc. Natl. Acad. Sci. U.S.A. 92*, 11578.
20. Unger, V. M., Hargrave, P. A., Baldwin, J. M., and Schertler, G. F. X. (1997) *Nature 389*, 203.
21. Yeagle, P. L., Alderfer, J. L., and Albert, A. D. (1997) *Biochemistry 36*, 9649.
22. Litman, B. J., and Mitchell, D. C. (1996) in *Biomembranes (*Lee, A., Ed.) Vol. 2A, pp 1−32, Jai Press, Greenwich, CT.
23. Mathews, R., Hubbard, R., Brown, P., and Wald, G. (1963) *J. Gen. Phys. 47*, 215.
24. Kibelbek, J., Mitchell, D. C., Beach, J. M., and Litman, B. J. (1991) *Biochemistry 30*, 6761.
25. Rath, P., Delange, F., DeGrip, W. J., Rothschild, K. J. (1998*) Biochem. J. 329*, 713.
26. Maeda, A., Ohkita, Y. J., Sasaki, J., Shichida, Y., and Yoshizawa, T. (1993) *Biochemistry 32*, 13267.
27. O'Brien, D. F., Costa, L. F., and Ott, R. A. (1977) *Biochemistry 16*, 1295.
28. Wiedmann, T. S., Pates, R. D., Beach, J. M., Salmon, A., and Brown, M. F. (1988) *Biochemistry 27*, 6469.
29. Gibson, N. J., and Brown, M. F. (1993) *Biochemistry 32*, 2438.
30. Mitchell, D. C., Straume, M., Miller, J. L., and Litman, B. J. (1990) *Biochemistry 29*, 9143.
31. Mitchell, D. C., Straume, M., and Litman, B. J. (1992) *Biochemistry 31*, 662.
32. Litman, B. J., and Mitchell, D. C. (1996) *Lipids 31*, s193.
33. Smith, H. G., Stubbs, G. W., and Litman, B. J. (1975) *Exp. Eye Res. 20*, 211.
34. Straume, M., Mitchell, D. C., Miller, J. L., and Litman, B. J. (1990) *Biochemistry 29*, 9135.
35. Mitchell, D. C., and Litman, B. J. (1998) *Biophys. J. 74*, 879.
36. Straume, M., and Litman, B. J. (1987) *Biochemistry 26*, 5113.
37. Johnson, M. L., and Frasier, S. G. (1985) *Methods Enzmol. 117*, 301.
38. Maeda, A., Ohkita, Y. J., Sasaki, J., Shichida, Y., and Yoshizawa, T. (1993) *Biochemistry 32*, 12033.
39. Attwood, P. V., and Gutfreund, H. (1980) *FEBS Lett. 119*, 323.
40. Lamola, A. A., Yamane, T., and Zipp, A. (1974) *Biochemistry 13*, 738.
41. Robinson, C. R., and Sligar, S. G. (1995) *Methods Enzyol. 259*, 395.
42. Chiou, J.-S., Tatara, T., Sawamura, S., Kaminoh, Y., Kamaya, H., Shibata, A., and Ueda, I. (1992) *Biochim. Biophys. Acta 1119*, 211.
43. Cao, Y., Varo, G., Chang, M., Ni, B. F., Needleman, R., and Lanyi, J. K. (1991) *Biochemistry 30*, 10972.
44. Fahmy, K., Jager, F., Beck, M., Zyyaga, T. A., Sakmar, T. P., and Siebert, F. (1993) *Proc. Natl. Acad. Sci. U.S.A. 90*, 10206.

BI990634M